Lab on a Chip

Cite this: DOI: 10.1039/c0lc00313a

www.rsc.org/loc

TECHNICAL NOTE

Multiplexed inkjet functionalization of silicon photonic biosensors†

James T. Kirk,‡[a] Gina E. Fridley,‡[a] Jeffrey W. Chamberlain,[a] Elijah D. Christensen,[a] Michael Hochberg[b] and Daniel M. Ratner*[a]

Received 18th August 2010, Accepted 26th January 2011
DOI: 10.1039/c0lc00313a

The transformative potential of silicon photonics for chip-scale biosensing is limited primarily by the inability to selectively functionalize and exploit the extraordinary density of integrated optical devices on this platform. Silicon biosensors, such as the microring resonator, can be routinely fabricated to occupy a footprint of less than 50 × 50 μm; however, chemically addressing individual devices has proven to be a significant challenge due to their small size and alignment requirements. Herein, we describe a non-contact piezoelectric (inkjet) method for the rapid and efficient printing of bioactive proteins, glycoproteins and neoglycoconjugates onto a high-density silicon microring resonator biosensor array. This approach demonstrates the scalable fabrication of multiplexed silicon photonic biosensors for lab-on-a-chip applications, and is further applicable to the functionalization of any semiconductor-based biosensor chip.

Introduction

Silicon photonics is revolutionizing the manipulation of light through the manufacture of nanometre-scale optical devices and integrated systems using the silicon-on-insulator (SOI) platform. Based on commercial CMOS fabrication, complex optical and electro-optical features can be integrated onto chip-scale devices for use in nonlinear optics, nano-optomechanics, gigahertz communications and biosensing.[1] In particular, silicon photonic biosensors have demonstrated sensitive label-free measurements for lab-on-a-chip applications including protein,[2,3] nucleic acid,[4] virus,[5] and bacterial[6] detection. These results have garnered particular attention for this new technology, as they demonstrate the potential for the chip-scale integration of complex biosensing functionality using existing silicon processes. However, these silicon fabrication techniques can produce sensor arrays with complexities and densities that cannot be easily exploited using traditional surface modification methods—necessitating a new approach for the multiplexed functionalization of dense arrays of microfabricated devices.

Silicon photonic biosensors, such as microtoroidal resonators,[7] liquid-core optical ring resonators,[8] and SOI microring resonators,[9,10] derive their remarkable sensitivity *via* a propagating optical mode that is confined to a microcavity. This mode is sensitive to changes in the local effective refractive index. Molecular interactions, such as the binding of proteins to the array surface, cause small changes in the local refractive index, resulting in a detectable shift in the resonance wavelength of the microcavity's optical mode.[11] Integrated optics are used to rapidly interrogate individual sensors, thereby monitoring the time-dependent changes in the refractive index of the surrounding media. Recently, SOI microring resonators (Fig. 1) have been used to detect antibody,[2] protein,[10] and nucleic acid[12] binding in real-time and are particularly well-suited for lab-on-a-chip applications.

For large-scale production of silicon photonic biosensors, reagent consumption, device density and printing throughput are major concerns. Presently, the reported method for multiplexed functionalization of microring resonator arrays utilizes microfluidic masking techniques.[13,14] This approach is limited by the sealing footprint to confine the fluidics and cannot achieve sufficient densities to exploit the potential complexity of silicon photonic biosensors. Thus, microfluidic masking limits the throughput of device functionalization while requiring relatively large volumes of reagent (tens to hundreds of microlitres) for multiplexed biosensing on the microring resonator array surface.

While pin-based contact printing has been used extensively for conventional microarray functionalization,[15,16] contact printing techniques have inherent limitations for the orthogonal modification of microring resonator-based arrays. Pin printing has high spot-to-spot variability, limited throughput, and most notably, contact by the pin can damage delicate silicon waveguides on the array surface.[17]

As a superior alternative to microfluidic masks or pin-based printing, non-contact piezoelectric (inkjet) printing has several

[a]*Department of Bioengineering, University of Washington, Box 355061, Seattle, WA, USA 98195. E-mail: dratner@u.washington.edu; Fax: +1 206-685-3300; Tel: +1 206-685-2840*
[b]*Department of Electrical Engineering, University of Washington, Box 352500, Seattle, WA, USA 98195*

† Electronic supplementary information (ESI) available: Materials and synthesis of glycoconjugates, Fig. S1 (schematic of the multi-chip holder) and Fig. S2 (scheme for glycoconjugate surface modification). See DOI: 10.1039/c0lc00313a

‡ Authors contributed equally.

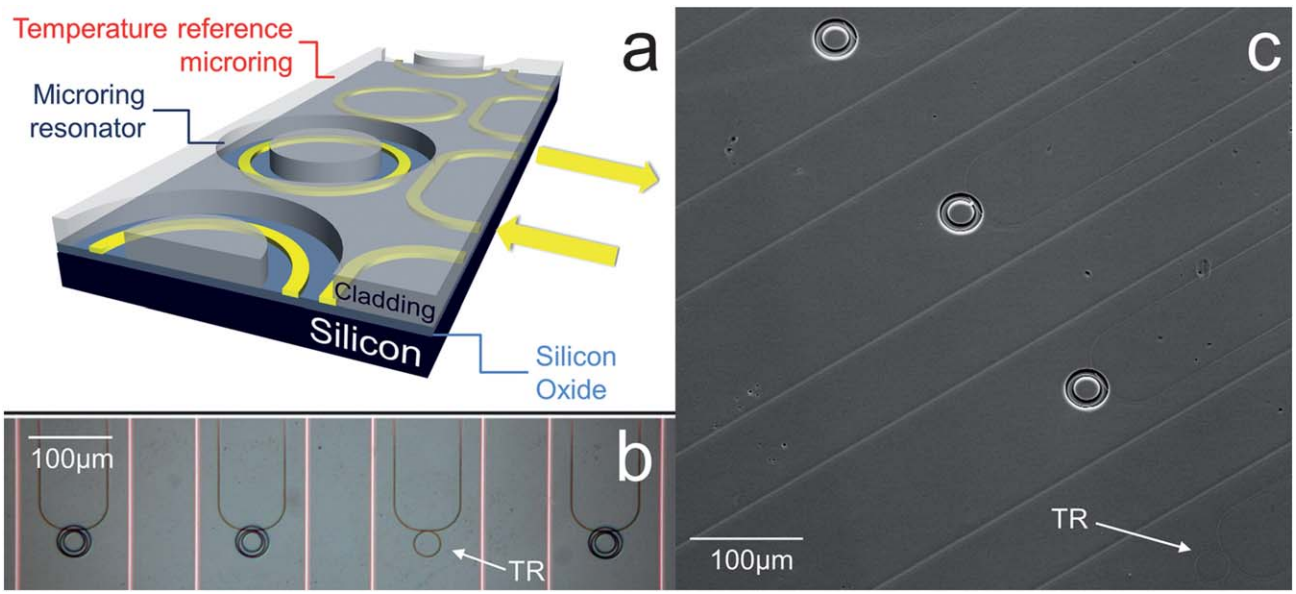

Fig. 1 (a) Three-dimensional depiction of several adjacent devices on a silicon photonic microring resonator biosensor array (not to scale). Light (yellow arrows) propagates through linear waveguides and the evanescent field couples into a microring resonator, confining the optical mode to the microcavity. Small changes in the local refractive index are detected as a shift in the resonance wavelength. A fluoropolymer-cladding covers the temperature reference control microring. The remaining microrings are suitable for chemical modification of the exposed silicon oxide surface. (b) A brightfield micrograph showing an array of silicon photonic microring resonator biosensors. Three of the pictured microring resonators are exposed for chemical functionalization and subsequent biosensing assays. A temperature reference (TR) control microring is indicated for clarity. (c) SEM micrograph showing an array of three exposed microrings and one temperature reference (TR) microring.

advantages for commercial-scale microarray fabrication.[17] Piezoelectric printers dispense highly reproducible picolitre-sized droplets from a fine glass capillary positioned above the substrate surface. The printing capillary expels sub-nanolitre volumes of sample, conserving precious reagent. The small droplet size, damage-free print mechanism, and fine positional control make piezoelectric printing ideal for rapid and multiplexed silicon microring resonator array modification.

This technical note describes a rapid, precise, and scalable method for the orthogonal printing of bioactive molecules on individual microring resonators using a piezoelectric non-contact printer. Bioactive glycoconjugates were selected for this proof of concept study as representative biomolecules—glycans are involved in a range of high-affinity and low-affinity binding events (including interactions with other carbohydrates, proteins, nucleic-acids, cells, bacteria, and viruses), and are highly stable to prolonged storage in ambient conditions.[18] The method described herein facilitates high throughput printing with minimal reagent consumption while retaining the bioactivity of the printed molecules. With the ability to chemically address individual microring biosensors, this approach opens the possibility of generating highly multiplexed arrays, composed of hundreds to thousands of simultaneous assays, on a square centimetre silicon chip.

Experimental

Silicon microring resonator biosensors and corresponding analysis instrumentation were manufactured by Genalyte, Inc. (San Diego, CA). The fabrication and use of these devices have been described previously.[2,10–12] The biosensor consists of an array of 32 individually addressable microring resonators (30 μm in diameter) suitable for real-time biosensing analysis. Of the 32 addressable sensors on each chip, 24 are exposed for biosensing and eight are coated with a fluoropolymer-cladding to serve exclusively as temperature and vibration reference controls (Fig. 1). With the exception of the exposed microring sensors, the entire chip is coated with the cladding, thereby minimizing waveguide losses and limiting all interactions with a biological sample to designated resonators. An external cavity diode laser with a center frequency of 1560 nm was rastered across the biosensor surface to rapidly interrogate individual microring resonators (approx. 250 ms per ring), measuring the shift in resonance wavelength of the optical cavity as a function of time. Materials and methods for the synthesis of bovine serum albumin (BSA)-conjugates, including BSA–mannose, BSA–galactose, BSA–lactose, and BSA–oligo(ethylene glycol) (BSA–OEG), are detailed in the ESI†. Briefly, thiolated sugars (mono-mannose, galactose, lactose residues) and thiolated oligoethylene glycol were attached to the free amines of BSA by way of the heterobifunctional cross-linker sulfo-SMCC (Pierce; Rockford, IL). BSA-glycoconjugates were passively adsorbed to the microring resonator biosensor surface upon printing by a piezoelectric non-contact printer.

Fabrication of the multi-chip holder

A 10 chip holder was designed in Autocad (AutoDesk, Inc., San Rafael, CA), and cut from a single layer of 10 mil polyethylene terephthalate (PET) (Fralock, Valencia, CA) with a 25 watt CO_2

laser (M-360, Universal Laser Systems, Inc., Scottsdale, AZ, USA) using previously published specifications.[19] External dimensions of the chip holder are $w = 165$ mm and $h = 39$ mm. Each chip slot is identical, $w_1 = 10$ mm, $w_2 = 6.06$ mm, $h_1 = 7$ mm and $h_2 = 3$ mm (Fig. 2b). Separation between chip slots is 10 mm. A schematic of the multi-chip holder is included in the ESI† (Fig. S1).

Rapid, multiplexed printing of bioactive reagents on silicon microring resonator devices

Reagents were deposited onto silicon devices using a Scienion S3 Flexarrayer (BioDot, Irvine, CA) piezoelectric non-contact printer. Piezo pulse and voltage parameters were set to the manufacturer's recommendations specific to the nozzle used (PDC80; optimized during production). The frequency of droplet release was 500 Hz. This method yielded reproducible and stable droplet formation for a given reagent solution. Droplet volume is dependent on the solution properties such as viscosity and surface tension, and ranged from 350 pL to 365 pL for the reagents used (as determined using the on-board CCD camera).

The multi-chip holder was aligned at the front left corner of the printer substrate support vacuum platform, flush with raised metal stops along the edges (Fig. 2a). Using the printer's accompanying software, specific print targets were defined within the pre-established coordinate space (approx. 1 μm spatial resolution); print target locations were referenced from the front left corner of the vacuum platform. Coordinates of individual microring resonators were determined using the dimensions of the multi-chip holder and the known position of individual ring resonators on each silicon chip (Fig. 2b). Initially, microspots of AlexaFluor488-conjugated streptavidin (AF488 SA) were printed to calibrate the piezoelectric non-contact printer (Fig. 2c and 3). Subsequently, printed spot precision was approximately 5 μm. The spotting accuracy was confirmed using a Nikon SMZ1500 fluorescence stereoscopic zoom microscope (Nikon, Inc.; Melville, NY). Images for publication were obtained using a Nikon Eclipse TE2000-U fluorescence microscope for composite brightfield/fluorescence images and a Zeiss Axiotron Z04-11 for high-magnification brightfield images.

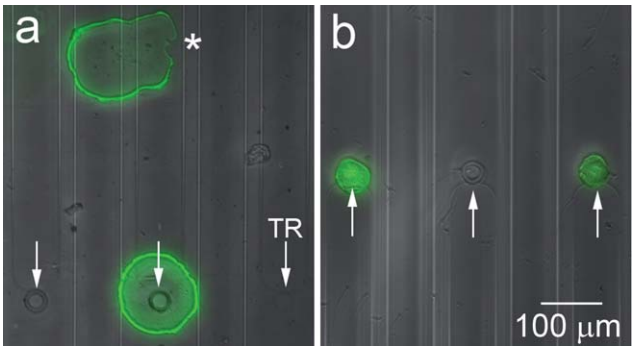

Fig. 3 (a) Fluorescence micrograph detailing the initial printer calibration. Upon visual inspection of inaccurately printed spots (*), printer software settings were modified to target a specific microring of interest. Following printer calibration, AF488 SA was printed on selected microrings. Note: a temperature reference (TR) microring has been identified for clarity. (b) An array of microrings (arrows) demonstrating the printing method's accuracy following calibration.

Real-time, multiplexed, label-free biosensing using silicon microring resonators

Functionalization layouts using the piezoelectric non-contact printer and BSA-glycoconjugates are detailed schematically in Fig. 4. Following printing, sensor chips were blocked with BSA (0.1% w/v, PBS running buffer, pH = 7.4) for one hour and rinsed thoroughly with PBS prior to biosensing experiments. Thirty-two microring resonators, including the eight fluoropolymer-clad thermal control rings, were analyzed across two microfluidic channels separated by a laser cut gasket (Genalyte, Inc.; San Diego, CA). Driven by negative-pressure syringe pumps (10 μL min^{-1}), the microfluidics were used to flow analyte over sets of 16 microring resonators per channel. Respective analyte concentrations were as follows: ConA = 200 nM, RCA = 500 nM, GRFT = 1 μM.

Results and discussion

The piezoelectric printer was initially calibrated using fluorescent protein conjugates to ensure reliable, efficient, and precise reagent deposition onto select microring resonators.

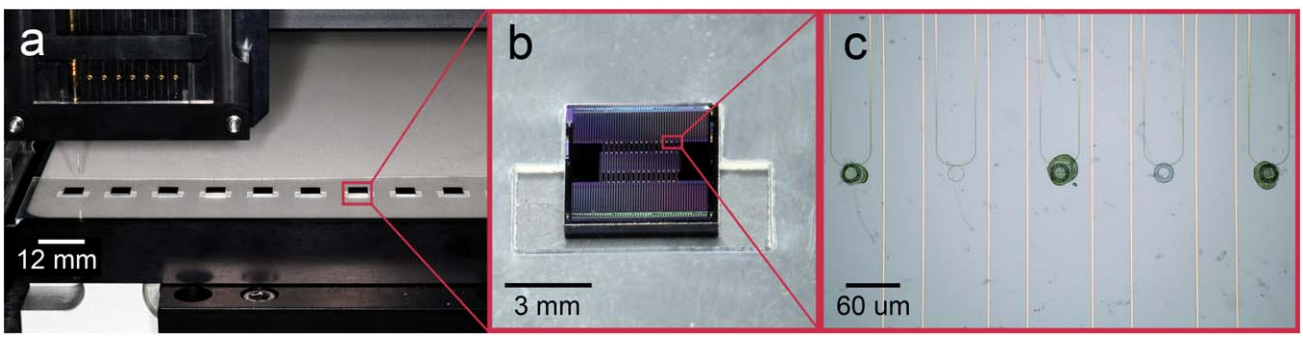

Fig. 2 (a) The non-contact printing setup. The multi-chip holder is precisely aligned on the printer's vacuum stage to ensure accurate reagent deposition across ten silicon photonic microring resonator biosensor arrays. (b) Photograph of a single silicon photonic biosensor chip aligned in the multi-chip holder. (c) Brightfield micrograph of an array of microring resonator devices. Following printer calibration, AlexaFluor488 streptavidin was reproducibly printed on specified microrings with a high degree of accuracy and precision.

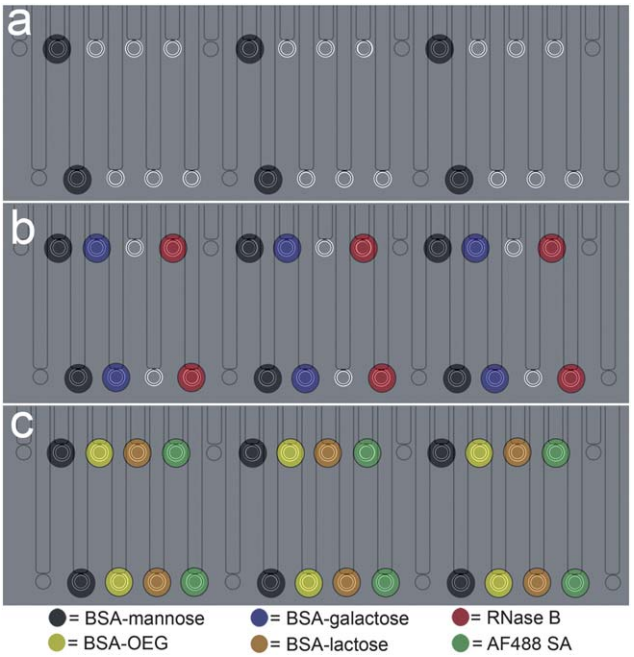

Fig. 4 Schematic representations of functionalized microring resonator arrays for biosensing demonstrations (not to scale). (a) Six non-adjacent microrings were printed with BSA–mannose to assess the bioactivity of printed glycoconjugates. (b) Six non-adjacent microrings were printed with BSA–mannose, BSA–galactose, or RNase B to evaluate ring-to-ring contamination during functionalization. (c) Six non-adjacent microrings were printed with BSA–mannose, BSA–lactose, or BSA–OEG glycoconjugates. Multiplexed detection was demonstrated using both GRFT and RCA lectins.

Subsequently, we tested the bioactivity of printed BSA-glycoconjugates using the model carbohydrate-binding protein (lectin), concanavalin A (ConA) and went on to demonstrate a multiplexed silicon photonic-based biosensor capable of detecting two lectins of interest, griffithsin (GRFT) and ricin (RCA). GRFT is a potent antiviral lectin isolated from the red algae *Griffithsia* sp. and has shown promising activity against human immunodeficiency virus (HIV) and severe acute respiratory syndrome (SARS)—these antiviral properties are attributed to its multivalent mannose-dependent binding capability.[20,21] RCA is a highly toxic galactose- and lactose-binding lectin[22] and is considered a potential biothreat agent.[23]

Calibration of the piezoelectric non-contact printer

Printing of fluorescently labeled proteins on individual microring resonators allowed visual verification of spotting accuracy using fluorescence microscopy. Positional inaccuracies in print location were corrected manually within the printer's software settings (Fig. 3).

These 'sighting in,' or calibration, results demonstrate that piezoelectric non-contact printers are suitable for printing reagents on individual microrings, and that the print location can be calibrated by visual inspection and subsequent software-based adjustments. This process requires that the printer's piezo settings be optimized to yield stable and uniform droplet formation prior to printer calibration. Additionally, biosensor chips must be carefully positioned on the printer's vacuum stage, as inconsistencies in device placement can introduce large errors in the location of printed reagents on the silicon chip, possibly even missing the sensing devices entirely. Therefore, precise machining of the multi-chip holder is necessary to ensure that all devices are correctly positioned on the printer stage.

To demonstrate the high-throughput capabilities for the deposition of biomolecules *via* this method, we concurrently printed ten chips with AF488 SA using the multi-chip holder. The printing nozzle was scanned across all ten chips while depositing AF488 SA —approximately 350 pL per spot—on six evenly spaced microrings per chip. Print accuracy and precision were confirmed using fluorescence microscopy, establishing that all chips were properly printed (results not shown). Remarkably, all ten silicon microring array chips were printed in a total of 9 seconds and consumed less than 25 nL of reagent. These results conclusively demonstrate the suitability of this printing method for rapid and efficient mass-production of densely functional microring resonator arrays. Furthermore, the efficiency can be increased with additional printing nozzles for simultaneous deposition of multiple biomolecules.

Detection of carbohydrate-binding proteins using printed glycan microring biosensor arrays

To establish this approach for multiplexed printing of bioactive molecules onto a microring resonator array, we have initially elected to explore several carbohydrate–protein interactions on a single chip. This category of glycan-mediated interactions is particularly relevant to the growing field of glycomics, which is employing the carbohydrate microarray to unravel the biological roles played by glycans in nature. Extending the potential sensitivity and scalability of silicon photonics arrays towards glycomics investigation will be particularly useful for glycan-based drug discovery and vaccine design.

To assess this printing technique for biosensing, we evaluated the bioactivity of printed BSA-glycoconjugates using a number of lectins. After "sighting in" the non-contact printer, BSA–mannose was deposited on non-adjacent microring resonators (Fig. 4a). The bioactivity of mannose-functionalized microrings was probed using the lectin ConA (Fig. 5a). ConA binding to BSA–mannose-functionalized microrings resulted in a maximum resonance shift of approximately 124.9 ± 3.8 pm ($n = 3$). This binding response indicates that BSA-glycoconjugates were specifically deposited on microring resonators and retained their intrinsic biological activity, validating the printing technique for biosensor surface modification.

A major challenge for multiplexed biosensor printing is the accurate deposition of reagent onto specific sensing elements within the array—in this case, individual microring resonators—without mislabeling neighboring devices. Spotting inaccuracy can result in poor array performance due to inhomogeneous modification of individual rings or cross-reactivity of adjacent sensors. To ascertain whether our printing method can address this challenge, we printed three different glycoconjugates onto alternating devices (Fig. 4b). Again, we utilized the mannose-binding lectin ConA to probe the bioactivity of the printed biomolecules, as shown in Fig. 5b. As expected, microrings functionalized with BSA–mannose and the natural

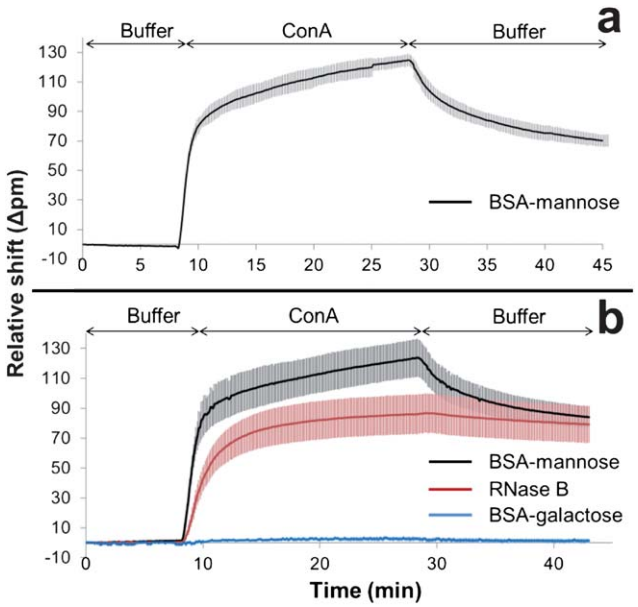

Fig. 5 After establishing a baseline signal in buffer, BSA-glycoconjugate-functionalized microring resonators were exposed to ConA, and then returned to buffer to observe ConA dissociation. (a) ConA (200 nM) binding to BSA–mannose-functionalized microring resonators, demonstrating the bioactivity of printed glycoconjugates. (b) ConA (200 nM) was flowed over an array of microring resonators functionalized with BSA–mannose, BSA–galactose, and RNase B. The binding responses show specific ConA binding to mannose-presenting biomolecules with no contamination of adjacent microrings. All data are presented as the average ± standard deviation, $n = 3$. BSA–mannose and RNase B binding data are normalized to unmodified microrings. BSA–galactose microrings are normalized to temperature reference control microrings.

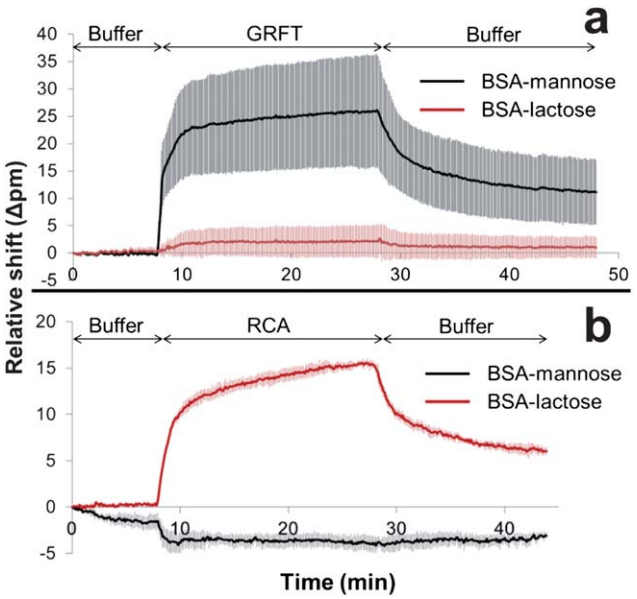

Fig. 6 After establishing a baseline signal in buffer, BSA-glycoconjugate-functionalized microring resonators were exposed to lectin, and then returned to buffer to observe lectin dissociation. (a) GRFT (1 μM) binding to BSA–mannose functionalized microring resonators. BSA–lactose functionalized microrings show minimal non-specific binding. (b) Specific RCA (500 nM) binding to BSA–lactose functionalized microrings. All data are presented as the average ± standard deviation, $n = 3$ and are normalized to BSA–OEG functionalized microring resonators.

mannosylated protein RNase B showed substantial relative shifts of 123.8 ± 12.7 pm ($n = 3$) and 86.6 ± 13.0 pm ($n = 3$), respectively. The BSA–galactose negative control microrings displayed a negligible binding response to ConA, as predicted by ConA's carbohydrate specificity.

Having confirmed the functionality of the printed glycan array using ConA, we prepared a model array to examine the carbohydrate-mediated interactions of GRFT and RCA (Fig. 4c). Microrings were printed with BSA–mannose and BSA–lactose. Subsequent binding was normalized to inert BSA–OEG functionalized microrings to control for non-specific protein interactions to the surface and the linker used for glycan/BSA conjugation (Fig. S2, ESI†).

GRFT binding to BSA–mannose modified microrings resulted in a maximum relative shift of 26.1 ± 10.3 pm ($n = 3$; Fig. 6a). While GRFT-binding to BSA–mannose is considerably lower than that of ConA, it is easily resolvable from the non-specific interactions to BSA–lactose printed as a control (2.6 ± 2.7 pm, $n = 3$). RCA binding was specific to BSA–lactose functionalized microrings, resulting in a relative shift of 15.5 ± 0.5 pm ($n = 3$; Fig. 6b). These promising results demonstrate excellent ring-to-ring selectivity based on printed glycoconjugates and strongly support the application of multiplexed silicon photonic biosensor arrays for glycomics applications. Additionally, the observed biosensor response opens the possibility of future study of the relative affinities of carbohydrate-binding proteins as well as surface glycan density. Additional effort is also underway to investigate the role of microring surface chemistries on the bioactivity of immobilized proteins and glycoproteins, with an emphasis on optimizing presentation of immobilized biomolecules.

Conclusions

Multiplexed silicon photonic biosensors have been limited by the throughput and functional density of current surface modification techniques for SOI devices. To fully exploit the device density and scalability inherent in silicon photonic integrated circuits, new methods for surface functionalization are required. This study described the facile multiplexed functionalization of a silicon microring biosensor array using a piezoelectric non-contact printer. Utilizing fluorescently labeled protein, a commercial piezoelectric printer was visually calibrated for the precise chemical modification of individual microring resonators on a silicon biosensor chip. This printing method was validated using a series of well-known carbohydrate–protein interactions, thereby confirming the bioactivity of printed biomolecules on multiplexed silicon biosensor arrays. Non-contact printing is an essential step towards realizing the full lab-on-a-chip potential of SOI label-free biosensing technologies.

Acknowledgements

This work was supported by NSF CBET (award no. 0930411) and the Washington Research Foundation and NSF MRSEC

(GEMSEC, award no. 0520567). MH would like to thank Gernot Pomrenke, at the Air Force Office of Scientific Research, for his support through an AFOSR Presidential Early Career Award in Science and Engineering grant. GEF gratefully acknowledges the NIH (EB000252) for support, JWC wishes to thank the NSF graduate research fellowship program, and EDC's contribution was sponsored by the NSF REU 'Hooked on Photonics' (award no. 0851730). The authors wish to thank Dr Paul Yager for generously providing access to the non-contact piezoelectric printer as well as Mr Anthony Au, Mr Tim Chang, and Ms Lauren Cummings for their assistance with fluorescence and SEM microscopy. In addition, the authors thank Dr Barry O'Keefe (NCI-Frederick, NIH) for his generous gift of griffithsin.

References

1 M. Hochberg and T. Baehr-Jones, *Nat. Photonics*, 2010, **4**, 492–494.
2 M. S. Luchansky and R. C. Bailey, *Anal. Chem.*, 2010, **82**, 1975–1981.
3 F. Vollmer, D. Braun, A. Libchaber, M. Khoshsima, I. Teraoka and S. Arnold, *Appl. Phys. Lett.*, 2002, **80**, 4057–4059.
4 J. D. Suter, I. M. White, H. Zhu, H. Shi, C. W. Caldwell and X. Fan, *Biosens. Bioelectron.*, 2008, **23**, 1003–1009.
5 F. Vollmer, S. Arnold and D. Keng, *Proc. Natl. Acad. Sci. U. S. A.*, 2008, **105**, 20701–20704.
6 A. Ramachandran, S. Wang, J. Clarke, S. J. Ja, D. Goad, L. Wald, E. M. Flood, E. Knobbe, J. V. Hryniewicz, S. T. Chu, D. Gill, W. Chen, O. King and B. E. Little, *Biosens. Bioelectron.*, 2008, **23**, 939–944.
7 A. M. Armani, R. P. Kulkarni, S. E. Fraser, R. C. Flagan and K. J. Vahala, *Science*, 2007, **317**, 783–787.
8 H. Y. Zhu, I. M. White, J. D. Suter, P. S. Dale and X. D. Fan, *Opt. Express*, 2007, **15**, 9139–9146.
9 A. Yalcin, K. C. Popat, J. C. Aldridge, T. A. Desai, J. Hryniewicz, N. Chbouki, B. E. Little, O. King, V. Van, S. Chu, D. Gill, M. Anthes-Washburn and M. S. Unlu, *IEEE J. Sel. Top. Quantum Electron.*, 2006, **12**, 148–155.
10 A. L. Washburn, L. C. Gunn and R. C. Bailey, *Anal. Chem.*, 2009, **81**, 9499–9506.
11 M. Iqbal, M. A. Gleeson, B. Spaugh, F. Tybor, W. G. Gunn, M. Hochberg, T. Baehr-Jones, R. C. Bailey and L. C. Gunn, *IEEE J. Sel. Top. Quantum Electron.*, 2010, **16**, 654–661.
12 A. J. Qavi and R. C. Bailey, *Angew. Chem., Int. Ed.*, 2010, **49**, 4608–4611.
13 A. L. Washburn, M. S. Luchansky, A. L. Bowman and R. C. Bailey, *Anal. Chem.*, 2010, **82**, 69–72.
14 C. F. Carlborg, K. B. Gylfason, A. Kazmierczak, F. Dortu, M. J. B. Polo, A. M. Catala, G. M. Kresbach, H. Sohlstrom, T. Moh, L. Vivien, J. Popplewell, G. Ronan, C. A. Barrios, G. Stemme and W. van der Wijngaart, *Lab Chip*, 2010, **10**, 281–290.
15 M. Seidel and R. Niessner, *Anal. Bioanal. Chem.*, 2008, **391**, 1521–1544.
16 E. J. Cho and F. V. Bright, *Anal. Chem.*, 2002, **74**, 1462–1466.
17 T. Tisone and J. Tonkinson, in *Protein Microarrays*, ed. M. Schena, Jones and Bartlett Publishers, Sudbury, MA, 2005, ch. 10, pp. 169–177.
18 A. Varki, *Essentials of Glycobiology*, Cold Spring Harbor Laboratory Press, Cold Spring Harbor, NY, 2009.
19 A. Hatch, A. E. Kamholz, K. R. Hawkins, M. S. Munson, E. A. Schilling, B. H. Weigl and P. Yager, *Nat. Biotechnol.*, 2001, **19**, 461–465.
20 T. Mori, B. O'Keefe, R. n. Sowder, S. Bringans, R. Gardella, S. Berg, P. Cochran, J. Turpin, R. J. Buckheit, J. McMahon and M. Boyd, *J. Biol. Chem.*, 2005, **280**, 9345–9353.
21 N. Ziółkowska, B. O'Keefe, T. Mori, C. Zhu, B. Giomarelli, F. Vojdani, K. Palmer, J. McMahon and A. Wlodawer, *Structure*, 2006, **14**, 1127–1135.
22 S. Olsnes and A. Pihl, *Biochemistry*, 1973, **12**, 3121–3126.
23 T. Nagatsuka, H. Uzawa, I. Ohsawa, Y. Seto and Y. Nishida, *ACS Appl. Mater. Interfaces*, 2010, **2**, 1081–1085.

